



Study of Antibiotics Adsorption onto the Binary of Oxide Mixtures System of Goethite and MnO₂

MAHAMADOU KAMAGATE^{1*}, TRAORE LANCINÉ¹,
COULIBALY GNOUGON NINA¹ and COULIBALY LACINA²

¹Department of Chemical Engineering, Faculty of Engineering and Technology,
University of Man, BP 20 Man, Cote d'Ivoire.

²Faculty of Science and Environmental Mangement, Université NANGUI ABROGOUA,
BP 01 BP 801 Abidjan 01, Cote d'Ivoire.

*Corresponding author E-mail: lancine.traore@univ-man.edu.ci

<http://dx.doi.org/10.13005/ojc/410510>

(Received: September 01, 2025; Accepted: October 15, 2025)

ABSTRACT

In the environment, adsorption is important for the movement and fate of organic pollutants. The study investigates the oxide mixture impact (i.e., MnO₂ and α -FeOOH) on the adsorption of Flumequine (FLU), with a view to simulating soil heterogeneity. Demonstration of FLU binding to these particle surfaces was achieved using batch sorption experiments, HPLC analyses, and ATR-FTIR spectroscopy. We investigated how synthetic α -FeOOH and MnO₂ particle surfaces interact to understand that affects FLU adsorption at different NaCl concentrations. ATR-FTIR results revealed the establishment of a metallo-bonded complex from neutral to acidic pH and a highly H-bonded complex at basic pH. We note strong attraction between FLU and MnO₂ due to the lower zero charge/ isoelectric point of this mineral (2.3-2.5) compared to goethite (8.9-9.5). Therefore, the FLU adsorption onto solids is as follows: α -FeOOH+MnO₂ > MnO₂ > α -FeOOH, with a percentage yield of 42%, 39%, and 36%, respectively, suggesting a slight superiority for the solid mixture.

Keywords: Flumequine, Adsorption, Oxide mixture, Goethite and MnO₂

INTRODUCTION

Recent years have seen an increasing body of evidence suggesting that antibiotics commonly used in human and animal medicine are being released into the environment¹. Fluoroquinolones (FQs) represent a group of powerful antibiotic medications that are widely employed in both human and veterinary medicine². Flumequine (FLU) is a non-natural quinolone frequently applied in aquaculture

as a preventive measure against diseases³. In addition, it was demonstrated to be highly efficacious in the treatment of urinary, pulmonary and digestive tract infections. Furthermore, studies have indicated that it is active against certain *Gram-positive* and *Gram-negative* micro-organisms⁴. The issue of bioavailability is of particular concern in this context, since it may result in elevated levels of FLU residues in the aquatic ecosystem⁵. Conversely, the elimination of FLU from wastewater by standard



treatment facilities is frequently found to be deficient⁶, and the presence of these compounds in the environment is frequently observed, and there is a possibility that they may have a deleterious effect on aquatic and terrestrial organisms⁷. Previously, several treatments have been reported such as biodegradation^{8,9}, photodegradation¹⁰, and adsorption to minerals in soils and sediments¹¹ of FLU. In the natural world, FLU's movement and fate are mostly controlled by its association with particles. This association is down to things being taken up by the organic fraction of soils and sediments in the watershed. Otherwise, MnO₂ can be joined up with other oxides as either single particles or coverings in soils and sediments¹². Other research has suggested that two different metal oxides that are present together, they are capable of experiencing heteroaggregation, a process which has the capacity to influence the sorption ability of the oxides by effectuating alterations to their surface charges and the number of surface sites¹³. This absence of correlation between research emphasis and environmental imperatives is primarily attributable to the intricacies inherent in operating within natural systems, a factor that is likely to impose substantial constraints on the ability to extrapolate research findings from rudimentary prototype systems to complex real-world environmental systems.

The aim of this study is to assess the impact of binary systems (MnO₂+Goethite) on FLU elimination. In addition to the kinetic experiments conducted on FLU in various combinations, a range of other experiments and calculations were performed. These encompassed the following: (i) the measurement of the surface charges of each oxide when tested individually and in a mixture of MnO₂ and goethite, (ii) the Attenuated Total Reflectance Fourier-Transform Infrared spectroscopy (ATR-FTIR) analysis of FLU sorbed on individual oxide and their mixtures, (iii) the sedimentation of each oxide and their mixture versus FLU concentration, and (iv) the FLU sorption on single oxide, and their binary mixture.

MATERIAL AND METHODS

Chemical products

The chemicals utilized in this study were of analytical grade or higher, procured from Sigma-Aldrich. A high-purity (99%) FLU starting solution was obtained through a dissolution process. This process

involved the dissolving of 52.4 mg (200 μmoles) of FLU in 10 mL of NaOH (1M), and subsequent dilution to 1 L of Ultra-Pure Water (UPW).

Synthesis and characterization of goethite and manganese dioxide particles

The synthesis of α-FeOOH and MnO₂ particles was conducted in accordance with the methodologies outlined in preceding studies^{14,15,16}. The particles obtained were subjected to a range of characterizations including size, BET specific surface area, nitrogen (N₂) adsorption measurements and composition chemical analysis. These were complemented by transmission electron microscopy (TEM) to provide comprehensive data on the morphology and composition of the particles. The specific surfaces of the synthetic α-FeOOH and MnO₂ are 85±0.1 and 374±3 m²/g, respectively.

Sorption experiments and UV-Visible spectrophotometry study

FLU solubility tests were performed in an effort to ascertain the effects of pH on the subject material. The experiments were carried out within 10 mM NaCl solutions, with solid FLU suspended in the solutions (~ 4-6 mg). We left the suspensions for 24 h to reach an equilibrium, then filtered the top layers (0.2 μm) and measured the FLU concentrations using a UV-Vis spectrophotometer (Varian). As we'll go through later, FLU is pretty insoluble at acidic pH (around 50 μM), which lines up with what other studies have found¹⁷.

MnO₂ (1.74 g/L, 650.76 m²/L) were utilized to realize different types of solutions in NaCl concentrations (10-1000mM). Goethite (24 g/L, 2040 m²/L) suspensions were prepared separately for each sample at the chosen ionic strength.

We carried out batch sorption experiments in different conditions, including reaction time, FLU concentration, pH and ionic strength, with a high amount of FLU at pH 4, with 10 mM of NaCl and 24 μM of FLU. They used an equal amount of goethite or MnO₂ and their mixture, with each solid having an area of 10 m²/L.

It should be noted that all batch tests were conducted in an atmosphere of N₂ (g) to guarantee the complete purging of dissolved CO₂ within the aqueous solutions. In fact, a solution of 24 μM

of FLU was prepared and subsequently added to goethite or MnO_2 (10 m^2/L) at the appropriate concentration of NaCl (i.e., 10, 500 or 1000 mM). Subsequently, the pH was regulated to the required value by adding of 0.1 M NaOH or HCl solutions. In a further experimental series, sorption isotherms were determined at $\text{pH} = 4.1 \pm 0.1$ and at $\text{pH} = 7.5 \pm 0.1$, for $[\text{FLU}]_{\text{tot}}$ concentrations varying from 1 to 150 μM in the presence of $\alpha\text{-FeOOH}$, MnO_2 , and their mixture at equal Surface Area. All solutions then underwent equilibration for a 24-h period, after which the supernatants were filtered (0.2 μm) prior to soluble FLU determination by UV-vis spectrophotometer at a wavelength of 246 nm. To verify the mass balance of FLU in the systems under study, desorption tests were conducted ($\text{pH}=12$).

The determination of FLU concentrations was accomplished by means of a high-performance liquid chromatography (HPLC, Waters 600 controller) system that was equipped with an automatic sampler (Waters 717 plus), a C18 column (250 $\text{mm} \times 4.6$ mm i.d., 5 μm), and a UV detector (246 nm, Waters 2489). The mobile phase was constituted of water and acetonitrile (60:40 v/v), with 0.1% formic acid. We set the flow rate at 1 mL/min in isocratic mode, as is standard practice in such experiments¹⁸.

ATR-FTIR spectroscopy

The experiment was conducted using a Nicolet IS50 spectrometer, a sophisticated piece of analytical equipment, which was utilized to record ATR-FTIR spectra within the 650-4000 cm^{-1} region. This instrument boasts a potassium bromide (KBr) crystal beam splitter and a total reflection (TCD) detector, both of which are crucial components in the precise measurement of infrared spectroscopy. Spectra of wet samples were acquired using a reflection diamond ATR module (i.e., DurasampIIR™, SensIR Technologies). The resolution of the single-beam spectrum was 4 cm^{-1} . Three sets of tests were carried out for the following: (i) the pH value is equal to 4, 6 and 7.5) with $[\text{FLU}]_{\text{tot}} = 50 \mu\text{M}$ and $[\text{NaCl}] = 10 \text{ mM}$ onto goethite, (ii) as well as MnO_2 , and (iii) an equal surface of goethite and MnO_2 mixture. Before being analyzed by ATR-FTIR, tubes from batch sorption experiments went through a 10,000 g centrifugation process for 30 minute. The application of wet mineral pastes to the ATR crystal was conducted in a direct and uniform manner. Subsequently, a lid was put on

the flowing-through cell to stop the water from evaporating.

Spectra were then systematically recorded. The reference spectra encompass those for pure water, as well as the filtered (0.2 μm) liquid from each batch adsorption test and FLU solid covered with a droplet of water to ensure more even application. Furthermore, a new reference spectrum was obtained from an aqueous FLU (FLU_{aq}) solution containing 10 mM of FLU in 1 M NaOH. This made sure there was enough FLU_{aq} for ATR-FTIR analysis. In addition, no evidence of FLU was found in any of the above samples due to its low solubility. It is noteworthy that the spectra presented herein pertain exclusively to the 1200-1800 cm^{-1} region.

Potentiometric proton titration (acid/base titration)

The titration process was conducted with the aid of an automated titrator (Titrand), manufactured by Metrohm, with the objective of measuring the oxides. Within the titrator cell, electrode measurements are computer controlled. The working solution was composed of 200 mL of ultrapure water and 0.12 g of goethite. In a subsequent series of tests, 0.02 g of MnO_2 and 0.059 g of goethite were utilized within the oxide mixtures. Conversely, 24 μM of FLU was added to the goethite and the oxide mixtures (i.e. MnO_2 + goethite). In order to avoid contamination from carbon dioxide (CO_2), the working solution for each oxide was purged with pure nitrogen gas (N_2). The adjustment of ionic strength was accomplished by employing a concentrated NaCl solution (2M) to attain concentrations of 10, 500, and 1000 mM, respectively. The pH was carefully regulated during the titrations process by the addition of precise solutions of HCl and NaOH, with concentrations of 0.1 mol/L and 0.04 mol/L, respectively. The pH and the potential redox (Eh) values were measured using two pH Metrohm electrodes, i.e. glass and reference¹⁹. Before calibrating the pH electrodes, it was necessary to carry out a blank titration of the standard electrolyte. The suspension was titrated by the addition of a defined volume of titrant and the subsequent measurement of the pH. Subsequent to each addition, a drift criterion for pH was utilized (mV/minute). We set a 30-min time limit for acquiring each data point. We used the same approach in the blank experiment¹⁹.

Sedimentation

Experiments were conducted to study the sedimentation of goethite-FLU, goethite-MnO₂-FLU and/or FLU at a pH of 4.0. The optical absorption at 508 nm was measured over time using a UV-vis spectrophotometer to monitor the tests^{20,21}. The equivalent surface area of the single oxide was 10 m²/L, and a derived from a reported method. For sedimentation measurement of goethite-manganese dioxide without FLU, different amount of MnO₂ was added, i.e., from 5 m²/L to 20 m²/L.

Otherwise for the sedimentation measurement of the oxide mixtures with FLU, the amounts of binary mixtures were maintained a total oxide concentration of 20 m²/L and concentration of FLU were varied to 8 to 100 μM. The solutions were mixed together and left for 24 h before the experiments. A 24 h time frame was selected for examination as the pre-equilibrium time when assessing the extent of aggregation in the mixtures. This time is commonly utilized prior to kinetic experiments, and the primary objective was to ascertain how the extent of aggregation influences MnO₂ reactivity. The utilization of light scattering techniques was precluded due to the broad spectrum of particle size distribution observed in the systems under investigation.

RESULTS AND DISCUSSION

Batch experiments

Kinetic batch tests were executed over a 5-day period, demonstrating that a steady-state condition was attained within 7 h of reaction time. Desorption tests further demonstrated that FLU was eliminated solely by sorption, with no evidence of breakdown by oxidation or other processes under the study's experimental conditions. Adsorption isotherms were determined for 10 and 50 μM solutions of FLU in a mineral suspension of density 10 m²/L (Fig. 1). These isotherms demonstrated a higher capacity for FLU loading on the mixture of MnO and goethite than on the separate systems (i.e., MnO₂ or α-FeOOH). As demonstrated in Fig. 1(a), at a pH below 5, approximately 36% of FLU was absorbed onto goethite. Conversely, Fig. 1(b) illustrates that an almost complete sorption was obtained on MnO₂ at pH of 4.5 (~39%). At a pH below 5, approximately 42% of the FLU was absorbed by the mixture of manganese dioxide and

goethite. The adsorption of FLU was observed to be optimal under acidic to circumneutral pH conditions, and least effective under basic conditions, as is also encountered in ligands. In addition, the negligible effect of NaCl concentration was observed, thereby indicating that FLU binding is likely to occur principally as strong metallic bond complexes associated with surface Fe sites and/or straight hydrogen bonds with surface hydroxyl groups. The ability of the latter to withstand changes in the strengthening of ions was clearly demonstrated by Johnson *et al.*,²². Conversely, poorer outer-sphere complexes are anticipated to be more susceptible to variations in ionic strength²³. This finding aligns with the observed adsorption phenomenon of FLU onto goethite wherein the impact of ionic strength proved to be insignificant across the concentration range of 1 mM to 100 mM of NaCl²⁴. The enhanced FLU loadings observed in MnO₂ can be attributed to two primary factors. Firstly, it is evident that the reactive site density of the MnO₂ under investigation is higher than that of goethite. However, the point of zero charge of MnO₂ (2-4.5)²⁵, is lower than that of goethite (7.5-9.4)^{14,26}. Secondly, at pH4, MnO₂ is predominantly net negative charged, with surface sites MnO⁻ and MnOH₀ being the most prevalent. It is hypothesized that geminal MnO groups of the plane of MnO₂ will be strongly reacted to cationic species. The number of sites per square nanometer is estimated to be 30.1, a value which may be indicative of an FLU removal mechanism that is more effective than goethite^{25,27}. In the case of the binary mixture of manganese dioxide+Goethite at pH <5, the sorption plateau is found to be higher for [FLU]_{tot} = 24 μM (~42%), as shown in Fig. 4(b). These results suggest that both phenomenal homo and heteroaggregation are contributing factors. Moreover, the empirical isotherm values are in close accordance with the kinetic batch uptake values at pH = 4.0. Within the system formed by the two oxides (MnO₂ and α-FeOOH), the charges are opposite, thus resulting in the occurrence of intensive heteroaggregation. This phenomenon subsequently led to the noticeable sedimentation of the particles (Fig. 4(a)). Adding 8-100 μM of FLU resulted in an average sedimentation rate of the mixture that was pretty similar to that of the control sample, i.e. the mixture without FLU. This phenomenon can be attributed to the presence of FLU, which leads to the formation of aggregates through both homo- and heteroaggregation processes. As demonstrated in

Fig. 4(b), the adsorption of FLU on α -FeOOH leads to a reduction in the charge of α -FeOOH, thereby diminishing its propensity for heteroaggregation with

MnO₂. Nevertheless, this process concomitantly fosters enhanced homoaggregation within α -FeOOH particles^{20,21}.

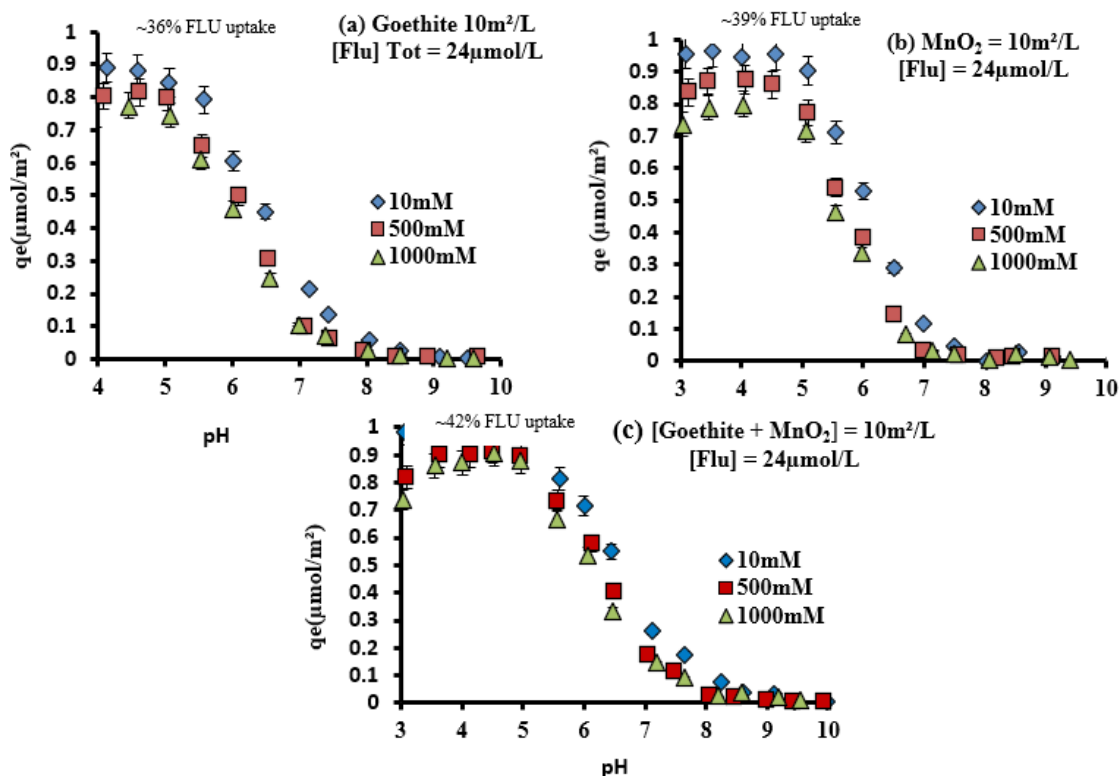


Fig. 1. FLU molecule adsorbed per m^2 ($[\text{FLU}]_{\text{sorbed}}$) for $[\text{FLU}]_{\text{tot}} = 24 \mu\text{M}$ on $10 \text{ m}^2/\text{L}$ goethite (a), MnO_2 (b) and $\text{MnO}_2 + \text{goethite}$ to equal surface (c) versus pH at different NaCl concentrations. The percentage of FLU uptake at the plateau is also given

Investigations using ATR-FTIR method

FLU_(s) and FLU_(aq) solutions

The ATR-FTIR spectra of the solid were utilized as a baseline for distinguishing surface-bound FLU species. Due to the relatively low solubility of FLU, band assignments in the soluble species were obtained from a 1 M NaOH solution (Fig. 2). The ATR-FTIR spectrum of FLU_(s) revealed three characteristic bands with maxima between 1410 and 1510 cm^{-1} . However, the bands in FLU_(aq) were shifted towards a longer wavelength by around 20 cm^{-1} . It has been established that these bands are attributable to C=C stretches ($\delta\text{C}=\text{C}$, ring) and C-H bends ($\delta\text{C}-\text{H}$, ring) in the aromatic and quinolone rings, respectively²⁸. The most significant distinction between the ATR-FTIR spectra of FLU_(s) and FLU_(aq) is the absence of two bands at 1710 and 1302 cm^{-1} , which occur as a result of the loss of a proton from the carboxyl groups. This process entails the elimination of the C=O and C-OH deformation

modes of the carboxylic group. The deprotonation process generates the 1395 and 1586 cm^{-1} bands, which are attributed to the symmetric ($\delta\text{COO},\text{s}$) and asymmetric ($\delta\text{COO},\text{as}$) stretching modes of the carboxylate, respectively. The difference between these bands, referred to as $\Delta\nu$, is equal to 191 cm^{-1} , calculated as $\delta\text{COO},\text{as} - \delta\text{COO},\text{s}$. Furthermore, these values are in accordance with those observed in earlier studies on (fluoro) quinolones, such as ciprofloxacin (CIP), which has been shown to assign $\delta\text{COO},\text{s}$ to a band within the 1360-1380 cm^{-1} range^{25,29,30}, and on ofloxacin (OFX) with a comparable peak at 1340 cm^{-1} ^{31,32}. Further analysis of the spectrum for FLU_(aq) revealed a distinct band at 1340 cm^{-1} . However, due to the reasons outlined subsequently, this band has not been assigned to COO,s . In contrast, the two absorption bands at 1263 and 1618 cm^{-1} are attributed to scissoring (bending) modes of the deprotonated carboxylate group (COO,sc) and to the bending of the quinolone ring carbonyl group ($\delta\text{C}=\text{O}$, carbonyl)¹⁷.

FLU-goethite

As illustrated in Fig. 2(a), the effect of pH on the ATR-FTIR spectra of 50 μM FLU reacted with 50 m^2/L goethite in 10 mM NaCl was demonstrated. Firstly, an analysis was conducted in order to observe both the characteristic features of $\text{FLU}_{(\text{s})}$ and $\text{FLU}_{(\text{aq})}$. The pH values at which FLU was investigated at 4.1 and 7.5. Specifically, the 1710 cm^{-1} band indicated the existence of protonated carboxylate groups, while the 1495 cm^{-1} band exhibited a shoulder on its high-energy side, implying the disruption of aromatic and/or quinolone rings due to intermolecular interactions. At pH values of 4.1 and 7.5, as evidenced by the spectra, the band at 1395 cm^{-1} for $\text{FLU}_{(\text{aq})}$ exhibits a significant decline, being almost completely replaced by a band centered at 1340 cm^{-1} . This finding lends further support to the hypothesis that the assignment of COO,s to the band at 1395 cm^{-1} in $\text{FLU}_{(\text{aq})}$ is accurate. It has been hypothesized that the COO band may be slightly purple-shifted (1590 cm^{-1}), which would result in a $\Delta\nu\approx 250$. This value would suggest that only one oxygen of the carboxylate binds to a surface Fe, indicating a monodentate coordination mode³³. The minor shift of $\delta\text{COO,sc}$ from 1263 to 1270 cm^{-1} offers further evidence for the involvement of the carboxylate in FLU surface complexation to goethite. A purple shift of 1618 cm^{-1} in the carbonyl ($\delta\nu\text{C}=\text{O}$) stretching mode of the carbonyl group ($\text{CN}=\text{O}$) is indicative of the implication of the keto group in the surface complex. This shift is in comparison to the $\text{FLU}_{(\text{aq})}$ or $\text{FLU}_{(\text{s})}$ carbonyl groups. A comparable transition from protonated $\text{FLU}_{(\text{s})}$ to $\text{Fe}(\text{FLU})_3(\text{s})$ has been documented in the preceding literature. In this instance, FLU establishes a bidentate deprotonated complex with Fe^{3+} via the keto group and one carboxylate oxygen³⁴.

FLU- MnO_2

We investigated how pH affects the way FLU- MnO_2 interacts with ionic strength using ATR-FTIR, and the results are shown in Fig. 2(b). When FLU reacts with MnO_2 , it causes big and consistent changes to its transmission FTIR spectrum (Fig. 2(b)). There's been a rise in the carbonyl stretch (1710 cm^{-1}), which is a sign of more protonated carboxyl groups in the solution, even though the pH has increased³³. This can be explained by the generation of slightly acidic carboxylic acids during the FLU reaction with MnO_2 , as evidenced by potentiometric titration (Fig. 3). As demonstrated

within the spectra, at pH 4.1 and 7.5, the band at 1395 cm^{-1} for $\text{FLU}_{(\text{aq})}$ almost completely disappears, being replaced by a band centered at 1340 cm^{-1} . This corroborates the attribution of COO groups to the band at 1395 cm^{-1} in $\text{FLU}_{(\text{aq})}$. It is important to note that the COO band may be slightly purple-shifted (1540 cm^{-1}), which gives a value of $\Delta\nu\approx 200\text{ cm}^{-1}$. This finding indicates that a single oxygen atom from the carboxyl group is capable of binding to a surface Fe atom, thereby suggesting a monodentate coordination mode³³. The minor shift of COO,sc from 1263 to 1250 cm^{-1} corroborates the hypothesis that the carboxylate is implicated in the surface complexation of FLU to MnO_2 . A purple shift of 1638 cm^{-1} in the carbonyl ($\nu\text{C}=\text{O}$) stretching mode of the carbonyl group is indicative of the involvement of the keto group in the surface complex. This shift is compared to that of the carbonyl group in the gas phase ($\text{FLU}_{(\text{aq})}$) or in a solid state ($\text{FLU}_{(\text{s})}$). A comparable transition from protonated $\text{FLU}_{(\text{s})}$ to $\text{Fe}(\text{FLU})_3(\text{s})$ has been documented in the past, wherein FLU establishes a bidentate deprotonated complex with Fe^{3+} via the keto group and a single carboxylate oxygen.

FLU- MnO_2 +goethite

The interactions between FLU and mixed oxides versus the pH under the same conditions were investigated, and the results are shown in Fig. 2(c). First, $\text{FLU}_{(\text{s})}$ and $\text{FLU}_{(\text{aq})}$ characteristics were also observed between pH 4.1 and 7.5. At different pH, the band at 1710 cm^{-1} were disappeared, that suggests the presence of protonated carboxylate groups, and the band at 1495 cm^{-1} possesses a shoulder on its high energy side suggesting the perturbation of aromatic and/or quinolone rings from intermolecular interactions. At pH = 4.11 and 7.36, the band at 1395 cm^{-1} for $\text{FLU}_{(\text{aq})}$ almost completely disappears and is replaced by a band centered at 1338 cm^{-1} . This further supports the assignment of COO,s to the band at 1395 cm^{-1} in $\text{FLU}_{(\text{aq})}$. The COO, as band might be slightly purple-shifted (1590 cm^{-1}), which gives $\Delta\nu\approx 252\text{ cm}^{-1}$, a value suggesting that a formation of stable Fe-carboxylate complexes on the oxide mixtures surface^{35,36,37}. The small shift of COO,sc from 1263 to 1270 cm^{-1} further points to the involvement of the carboxylate in FLU surface complexation to goethite¹⁷. A purple-shift of $\delta\text{C}=\text{O}$, carbonyl (1618 cm^{-1}) compared to $\text{FLU}_{(\text{aq})}$ or $\text{FLU}_{(\text{s})}$, also suggests the involvement of the keto group in the surface complex. A similar shift from

protonated FLU_(s) to Fe(FLU)₃(s) was previously reported, where FLU forms a bidentate deprotonated complex with Fe³⁺ through the keto group and one carboxylate oxygen³⁸.

Table 1: A summary table of characteristic peak versus oxides taken separately or as a mixture

Solids/Functional groups	α -FeOOH	MnO ₂	MnO ₂ and α -FeOOH
δ C=C, ring δ C-H, ring Symmetric (δ COO,s) Asymmetric (δ COO,as)	Aromatic and quinolone rings Disruption of aromatic and/or quinolone rings at 1495 cm ⁻¹ band and 1395 cm ⁻¹ band is replaced by 1340 cm ⁻¹ band, minor shift of COO,sc from 1263 to 1270 cm ⁻¹	Aromatic and quinolone rings Minor shift of COO,sc from 1263 to 1250 cm ⁻¹ , and COO groups to the band at 1340 cm ⁻¹ and may be slightly purple-shifted to 1540 cm ⁻¹	Aromatic and quinolone rings Band at 1395 cm ⁻¹ is completely disappears and replaced by 1338 cm ⁻¹ and COO, as band might be slightly purple-shifted to 1590 cm ⁻¹
δ C=O,carbonyl δ C-OH	Carboxylate groups at 1710 cm ⁻¹ bands	Complete disappearance of Carbonyl stretch at 1710 cm ⁻¹	Complete disappearance of Carbonyl stretch at 1710 cm ⁻¹
$\Delta\nu \approx \delta$ COO,as- δ COO,s	250 cm ⁻¹	200 cm ⁻¹	252 cm ⁻¹

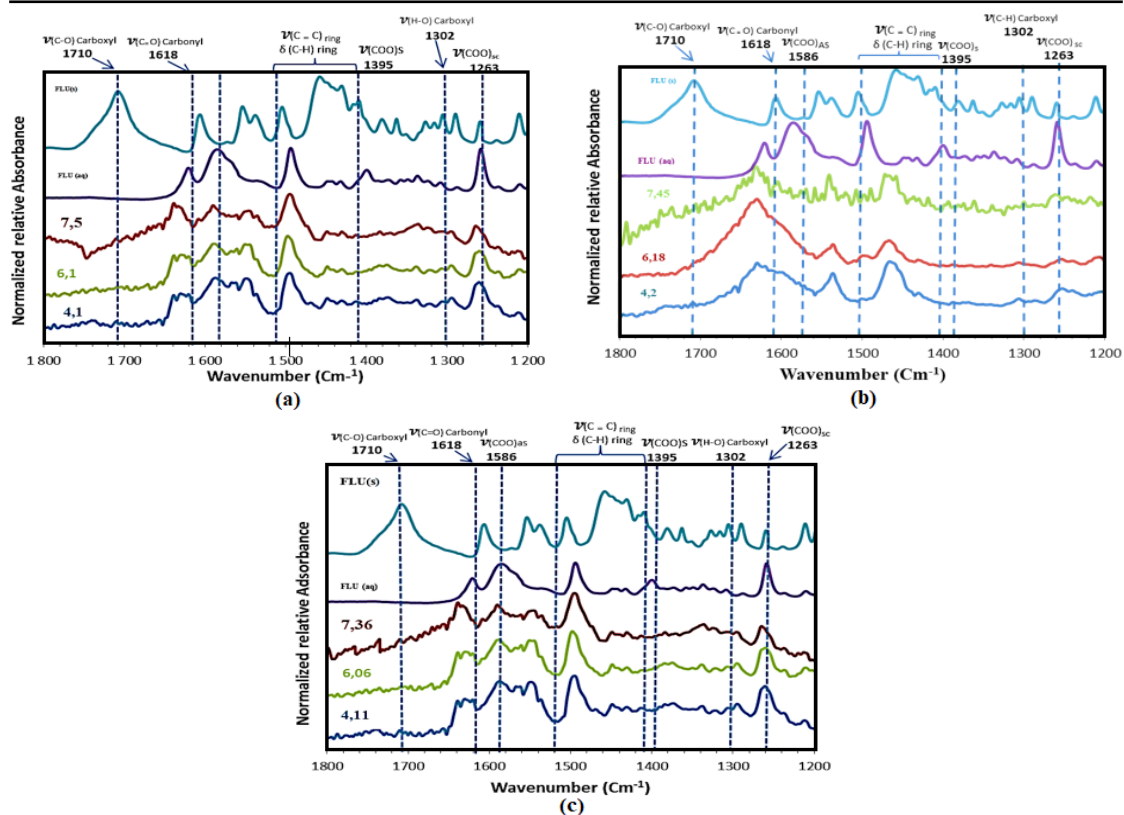


Fig. 2. ATR-FTIR spectra of FLU adsorbed to goethite (a) and MnO₂ (b), and goethite+MnO₂ (c) for various pH (pH=7.5, 6.1 and 4.1), [FLU]_{tot} = 50 μ M in 10 mM NaCl. ATR-FTIR spectra of dissolved FLU in 1 M NaOH (FLU_(aq)) and protonated FLU under its solid form (FLU_(s)) are shown as references.

Potentiometric proton titration (acid/base titration)

Figure 3 shows the results of the titration experiments of goethite and the oxide mixtures to equal surface with or without FLU. It was established that the MnO₂ was negatively charged at a pH of 4.0, given that its PZC was 2.3. For goethite, the pH PZC was observed at

pH 8.96. So, it's obvious that the surface charge of the oxides is really important in the adsorption process. Therefore, measuring the external charge of the oxide surfaces is important to enhance understanding of the adsorption mechanism. Furthermore, the effect of pH of the solution onto the FLU sorption was studied at pH 4 to pH10, with comparison to experiments developed at

the natural pH of FLU (pH 6.3). The pH PZC of oxide mixtures was observed to occur at an interval between pH 5.6 and 5.8. For the ternary mixture systems, a shift in pH PZC was evident at pH 4.68 (Fig. 3). In addition, an alteration in the pH of goethite+FLU was observed, with a shift to a value of 5.0 (see Fig. 3). It can thus be concluded that the substance exhibits only negligible acid properties for its carboxylic group and is deficient in piperazine ring properties^{18,35}. As a consequence, the neutral form of FLU is predominant at pH < pKa, while the anionic forms are prevalent at pH > pKa. We've figured out that, at pH values lower than the pH PZC, the oxides were positively charged, and the opposite was seen at higher pH values. The phenomenon of sorption appears to be diminished at the ranges of this pH.

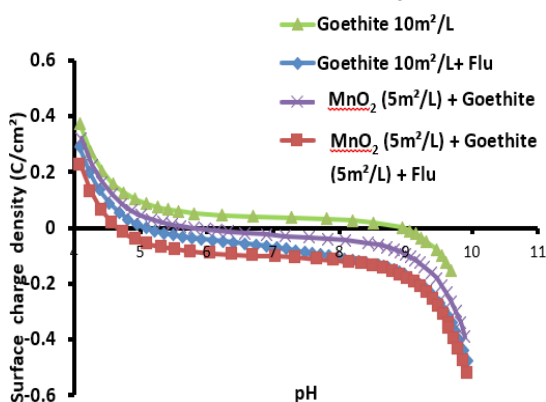


Fig. 3. Experimental of determinate charge surface in 10 mM NaCl versus pH. The results of the titration experiments of goethite and the oxide mixtures to equal surface with or without FLU were shown

Sedimentation rate

As illustrated in Fig. 4, the process of clumping together between the oxide particles in the system under investigation has been shown to reach a pseudo steady-state after a period of 7 h for the initial equilibrium. The objective of the sedimentation experiments was to ascertain the extent of the oxide particles joined together in groups, as opposed to measuring how quickly this happened. The results of the sedimentation analysis demonstrated a direct correlation between the increase in the amount of MnO₂ and the rise in the sedimentation rate. However, this sedimentation rate of goethite was less high than in mixture of goethite and MnO₂. For on other hand, the added of FLU on the oxide mixtures to equal surface increased more the sedimentation

rate. This behavior could be explained by the fact that when the concentrations of FLU increase, and the observed sedimentation was due to aggregates formed through both homo- and heteroaggregation. It is evident that the decline in the surface charge of goethite resulting from the adsorption of FLU would diminish its capacity for heteroaggregation with MnO₂. However, this process would concomitantly augment the extent of homoaggregation within the goethite particles. This observation was corroborated by Zhang *et al.*,²⁰ who reported analogous results when examining the effects of varying concentrations (0.2-2 mg-C/L AHA) of humic acid (AHA) on a mixture of goethite and MnO₂.

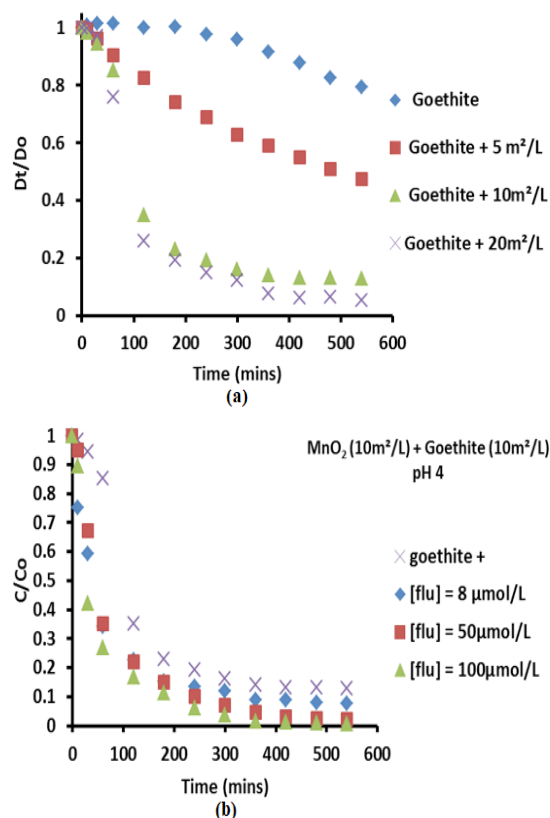


Fig. 4. Sedimentation rate of single goethite or with FLU (a) and goethite+MnO₂ or with FLU (b) versus time at pH = 4.0. Experimental conditions: For the tests of oxide heteroaggregations, [Goethite] = 10m²/L and the amounts of MnO₂ added were increased 5 to 20m²/L in 10 mM of NaCl. For the tests of homoaggregation, the various concentrations of FLU (8 to 100μM) were added on the mixture of 10m²/L goethite and 10m²/L MnO₂

CONCLUSION

Our studies of combined kinetic, charge surface, sedimentation rate, potentiometric proton

titration and ATR-FTIR investigations showed that FLU was eliminated by adsorption and without oxidation. Consequently, the findings of this study will contribute essential information that will facilitate the establishment of a connection between former model systems, in which only one oxide was included, and environmental systems, in which multiple oxides or minerals coexist. In order to achieve a mechanistic understanding of the role of MnO₂ within a complex soil system containing multiple constituents, including different metal oxides. It is therefore evident that this work demonstrated the manner in which the interactions between oxide mixtures impact precursor complex formation or adsorption. The development of predictive tools for the estimation of the adsorption and transportation of contaminants in soil and water environments stands to benefit significantly from these results, and will thus be a fruitful avenue for future research.

ACKNOWLEDGEMENT

This research was partially supported by the government of the Ivory Coast, through Campus France Company (contract C2D). We would like to express our gratitude to all the members of the research team for their contribution to the writing of this paper and for their technical and administrative support throughout the study, as well as for their experimental work.

Conflict of Interest

The authors state that they have no personal or professional interests that might affect their work.

Compliance with Ethical Standards

This article does not contain any studies involving human or animal subjects.

REFERENCES

1. Kummerer, K. Antibiotics in the aquatic environment-A review-Part I, *Chemosphere.*, **2009**, 75, 417–434.
2. Zhang, H.; Huang, C.-H. Adsorption and oxidation of fluoroquinolone antibacterial agents and structurally related amines with goethite., *Chemosphere.*, **2007**, 66, 1502–1512.
3. Mejías, C.; Santos, J. L.; Martín, J.; Aparicio, I.; Alonso, E. Automatised on-line SPE-chiral LC-MS/MS method for the enantiomeric determination of main fluoroquinolones and their metabolites in environmental water samples., *Microchem. J.*, **2023**, 185, 108217.
4. Rashid, A.; Muhammad, J.; Khan, S.; Kanwal, A.; Sun, K. Poultry manure gleaned antibiotic residues in soil environment : A perspective of spatial variability and influencing factors., *Chemosphere.*, **2023**, 317, 137907.
5. Sundararamana, S.; Kumar, A.; Deivasigamani, P.; Devarajan, Y. Emerging pharma residue contaminants: Occurrence, monitoring, risk and fate assessment – A challenge to water resource management., *Sci. Tot. Environ.*, **2022**, 825(15), 153897.
6. Williams, A. J.; Deck, J.; Freeman, J. P.; Chiarelli, P.; Adjei, M.; Heinze, M. D.; Sutherland, T. M. Biotransformation of flumequine by the fungus *Cunninghamella elegans*, *Chemosphere.*, **2007**, 67, 240–243.
7. Zhou, Y.; Li, W.-B.; Kumar, V.; Necibi, M. C.; Mu, Y.-J.; Shi, C.; Chaurasia, D.; Chauhan, S.; Chaturvedi, P.; Sillanpää, M.; Zhang, Z.; Awasthi, M. K.; Sirohi, R. Synthetic organic antibiotics residues as emerging contaminants waste-to-resources processing for a circular economy in China: Challenges and perspective., *Environ. Res.*, **2022**, 211, 113075.
8. Parshikov, I. A.; Freeman, J. P.; Lay, J. O. J.; Beger, R.D.; Williams, A. J.; Sutherland, J. B. Regioselective transformation of ciprofloxacin to N-acetylciprofloxacin by the fungus *Mucor ramannianus*, *FEMS Microbiol. Lett.*, **1999**, 177, 131–135.
9. Wetzstein, H.-G.; Stadler, M.; Tichy, H.-V.; Dalhoff, A.; Karl, W. Degradation of ciprofloxacin by basidiomycetes and identification of metabolites generated by the brown rot fungus *Gloeophyllum striatum*, *Appl. Environ. Microb.*, **1999**, 65, 1556–1563.
10. Knapp, C.W.; Cardoza, L.A.; Hawes, J.N.; Wellington, E.M.H.; Larive, C.K.; Graham, A.W. Fate and effects of enrofloxacin in aquatic systems under different light conditions., *Environ. Sci. Technol.*, **2005**, 39, 9140–9146.
11. Gu, X.; Tan, Y.; Tong, F.; Gu, C. Surface complexation modeling of coadsorption of antibiotic ciprofloxacin and Cu(II) and onto goethite surfaces., *Chem. Eng. J.*, **2015**, 269, 113-120.

12. Rodrigues-Silva, C.; Maniero, M.G.; Rath, S.; Guimaraes, J.R. Degradation of flumequine by the Fenton and photo-Fenton processes: Evaluation of residual antimicrobial activity., *Sci. Total Environ.*, **2013**, *445*(446), 337–346.
13. Nieto, J.; Freer, J.; Contreras, D.; Candal, R.J.; Sileo, E. E.; Mansilla, H. D. Photocatalyzed degradation of flumequine by doped TiO₂ and simulated solar light., *J. Hazard. Mater.*, **2008**, *155*, 45–50.
14. Gaboriaud, F.; Ehrhardt, J. J. Effects of different crystal faces on surface charge of colloidal goethite (α -FeOOH) particles: an experimental and modeling study, *Geochim., Cosmochim. Acta.*, **2003**, *67*, 967-983.
15. Laha, S.; Luthy, R. G. Oxidation of aniline and other primary aromatic amines by manganese dioxide., *Environ. Sci. Technol.*, **1990**, *24*, 363–373.
16. Murray, J. W. The surface chemistry of hydrous manganese dioxide., *J. Colloid Interface Sci.*, **1974**, *46*, 357–371.
17. Marsac, R.; Martin, S.; Boily, J-F.; Hanna, K. Oxolinic acid binding at goethite and akaganéite surfaces: experimental study and modeling., *Environ. Sci. Technol.*, **2016**, *50* (2), 660–668.
18. Sotelo, J. L.; Ovejero, G.; Rodriguez, A.; Alvarez, S.; Garcia, J. Analysis and modeling of fixed bed column operation on flumequine removal onto activated carbon: pH influence and desorption studies., *Chem. Eng. J.*, **2013**, *228*, 102-113.
19. Janot, N.; Reiller, P. E.; Zheng, X.; Croué, J.-P. Using Spectrophotometric Titrations To Characterize Humic Acid Reactivity at Environmental Concentrations., *Environ. Sci. Technol.*, **2010**, *44*(17), 6782-6788.
20. Zhang, H.; Tadjale, S.; Huang, J.; Lee, G-J. Effect of MON on Oxidative Reactivity of Manganese Dioxide in Binary Oxide Mixtures with Goethite or Hematite., *Langmuir.*, **2015**, *31*, 2790-2799.
21. Tadjale, S.; Zhang, H. Impact of interactions between Metal Oxides to Oxidative Reactivity of Manganese Dioxide., *Environ. Sci. Technol.*, **2012**, *46*, 2764-2771.
22. Johnson, B. B.; Sjöberg, S.; Persson, P. Surface Complexation of Mellitic Acid to Goethite: An Attenuated Total Reflection Fourier Transform Infrared Study., *Langmuir.*, **2004**, *20*, 823-828.
23. Zhang, H.; Chen, W.-R.; Huang, C.-H. Kinetic modeling of oxidation of antibacterial agents by manganese oxide., *Environ. Sci. Technol.*, **2008**, *42*, 5548–5554.
24. Paul, T.; Liu, J.; Machesky, M. L.; Strathmann, T. Adsorption of zwitterionic fluoroquinolone antibacterials to goethite: A charge distribution-multisite complexation model., *J. Coll. Int. Sci.*, **2014**, *428*, 63-72.
25. Tripathy, S. S.; Kanungo, S. B. Adsorption of Co²⁺, Ni²⁺, Cu²⁺ and Zn²⁺ from 0.5 M NaCl and major ion sea water on a mixture of δ -MnO₂ and amorphous FeOOH., *J. Colloid. Interf. Sci.*, **2005**, *284*, 30-38.
26. Boily, J.-F.; Lützenkirchen, J.; Blamès, O.; Beattie, J.; Sjöberg, S. Modeling proton binding at the goethite (α -FeOOH)–water Interface., *Colloids Surf. A.*, **2001**, *179*, 11–27.
27. Kanungo, S.B.; Tripathy, S.S.; Mishra, S.K.; Sahoo, R. B. Adsorption of Co²⁺, Ni²⁺, Cu²⁺ and Zn²⁺ onto amorphous hydrous manganese dioxide from simple (1-1) electrolyte solutions, *J. Colloid. Interf. Sci.*, **2005**, *284*, 30-38.
28. Neugebauer, U.; Szeghalmi, A.; Schmitt, M.; Kiefer, W.; Popp, J.; Holzgrabe, U. Vibrational spectroscopic characterization of fluoroquinolones., *Spectrochim. Acta, Part A.*, **2005**, *61*, 1505-1517.
29. Pei, Z.-G.; Shan, X.-Q.; Kong, J.-J.; Wen, B.; Owens, G. Co-adsorption of ciprofloxacin and Cu(II) on montmorillonite and kaolinite as affected by solution pH., *Environ. Sci. Technol.*, **2010**, *44*(3), 915-920.
30. Rakshit, S.; Sarkar, D.; Elzinga, E.J.; Punamiya, P.; Datta, R. Mechanisms of ciprofloxacin removal by nano-sized magnetite., *J. Hazard. Mater.*, **2013**, *246-247*, 221-226.
31. Goyne, K. W.; Chorover, J.; Kubicki, J. D.; Zimmerman, A. R.; Brantley, S. L. Sorption of the antibiotic ofloxacin to mesoporous and nonporous alumina and silica., *J. Coll. Int. Sci.*, **2005**, *283*, 160–170.
32. Paul, T.; Machesky, M.; Strathmann, T. Surface Complexation of the Zwitterionic Fluoroquinolone Antibiotic Ofloxacin to Nano-Anatase TiO₂ Photocatalyst Surfaces., *Environ. Sci. Technol.*, **2012**, *46*(21), 11896-11904.

33. Fang, N.; Xi, Y.; Zhang, J.; Wu, J.; Cheng, H.; He, Q. Insight into Adsorption Kinetics, Equilibrium, Thermodynamics, and Modeling of Ciprofloxacin onto Iron Ore Tailings., *Water*, **2025**, *17*, 760. <https://doi.org/10.3390/w17050760>.
34. Le Crom, S.; Boily, J.-F. Molecular-level insight into ciprofloxacin adsorption on goethite: I. Approach and non-specific binding, *Phys. Chem., Chem. Phys.*, **2025**, *27*, 4446-4456, DOI <https://doi.org/10.1039/D4CP04027A>
35. Paludo, D.; Bonfleur, E. J.; Melo, V. F.; Pasquali, G. D. L.; Bazoti, S. F.; Corrêa, R. S. Adsorption of ciprofloxacin on iron oxides in the absence or presence of polyethylene microplastic, *Colloids Surf. A Physicochem., Eng. Asp.*, **2025**, *711*, 136378, <https://doi.org/10.1016/j.colsurfa.2025.136378>.
36. Tolls, J. Sorption of veterinary pharmaceuticals in soils: A Review, *Environ. Sci. Technol.*, **2001**, *35*(17), 3397-3406.
37. Ludmilla, A.; Sposito, G. Complexes of the antimicrobial ciprofloxacin with soil, peat, and aquatic humic substances., *Environ. Toxicol. Chem.*, **2013**, *32*(7), 1467-1478.
38. Trivedi, P.; Vasudevan, D. Spectroscopic Investigation of Ciprofloxacin Speciation at the Goethite–Water Interface., *Environ. Sci. Technol.*, **2007**, *41*(9), 3153-3158.
39. Zhang, H.; Huang, C.-H. Oxidative transformation of triclosan and chlorophene by manganese oxides., *Environ. Sci. Technol.*, **2003**, *37*, 2421-2430.